

## Two-dimensional hydrodynamic focusing in a simple microfluidic device

Claire Simonnet and Alex Groisman<sup>a)</sup>

Department of Physics, University of California, San Diego, 9500 Gilman Drive, MC 0374, La Jolla, California 92093

(Received 12 May 2005; accepted 28 July 2005; published online 8 September 2005)

Two-dimensional flow focusing in pressure-driven flow is demonstrated in a microfluidic device made of a single cast of a silicon elastomer. A stream injected into the device is shaped to a variety of rectangular profiles. A flow of particles is focused into a thin layer with homogeneous velocity. A blob of dye injected into a microchannel is transported over a long distance with minimal dispersion. The device can be integrated into lab-on-a-chip systems and used as a low-cost flow cytometry chamber. © 2005 American Institute of Physics. [DOI: 10.1063/1.2046729]

Microscopic flows almost always occur at low Reynolds number ( $Re$ ), and are laminar and stable. Therefore, particles and molecules injected into them follow well defined streamlines. This allows efficient hydrodynamic focusing—a stream carrying the particles is squeezed by other streams into a narrow tube of flow with a uniform velocity.<sup>1</sup> Optical properties (e.g., light scattering and fluorescence) of the particles moving with the same velocity through a narrow region of space can be measured with high accuracy and high throughput, which is the basis of the modern flow cytometry.<sup>2</sup>

Much of the recent development in microscopic fluid dynamics is connected with the widespread use of lithographic micromachining and in particular with the introduction of soft lithography.<sup>3</sup> In this method, microfluidic devices are cast of polymer materials using microfabricated molds, dramatically reducing time and costs of production. Lithographically fabricated microfluidic devices normally have planar channel architectures. Hydrodynamic focusing in the plane of the device is straightforward and has been used to study kinetics of chemical reactions<sup>4</sup> and to deliver chemicals with high spatial resolution.<sup>5</sup> Nevertheless, planar microchannel networks generally do not allow out-of-plane focusing. Therefore, particles in the focused stream are still spread in the out-of-plane direction, and if the flow is driven by pressure and has a parabolic profile, their velocities are widely dispersed. These two factors are major complications for accurate flow cytometry in microfluidic devices.<sup>6</sup> The few microfluidic devices that achieved two-dimensional (2D) hydrodynamic focusing (in both in-plane and out-of-plane directions) required either laborious assembly<sup>7</sup> or individual fabrication,<sup>8</sup> which suggests high fabrication costs and limited fidelity, rendering their integration into lab-on-a-chip systems problematic.

In this paper, we describe a microfluidic device which focuses and shapes the profile of a stream in 2D and is made of a single cast of a silicon elastomer, polydimethylsiloxane (PDMS), sealed with a microscope cover glass. The device is shown in Fig. 1. The out-of-plane ( $z$ -direction) focusing is achieved by combining a tall-and-narrow central channel with two pairs of shallow channels connected to it on the sides at the bottom [Figs. 1(b) and 1(c)]. The tall-and-narrow channel has a depth of  $100\ \mu\text{m}$  and width of only  $16\ \mu\text{m}$ .

Therefore, the liquid flowing into it from  $8\ \mu\text{m}$  deep channels  $B$  and  $C$  is effectively injected from the bottom and pushes the liquid in the tall-and-narrow channel towards the top. The stream injected from channels  $B$ , which may carry particles or chemicals [Fig. 1(c)], becomes sandwiched in the  $z$ -direction between the streams from channel  $A$  and channels  $C$ . Streams from two channels  $E$  provide focusing in the  $y$ -direction (in-plane), and there is normally no flow through channels  $D$ .

Fabrication of the microfluidic device followed the standard soft lithography protocol described in detail elsewhere.<sup>3,9</sup> The master mold was fabricated in a two step procedure. First, a 4 in. silicon wafer was spin-coated with an  $8\ \mu\text{m}$  layer of an UV-curable epoxy (SU8-2005, MicroChem, Newton, MA) and exposed to UV-light through a specially designed photomask with a resolution of 20 000 dpi. Next the wafer was coated with  $100\ \mu\text{m}$  thick layer of the epoxy (SU8-2050), exposed through another photomask and developed. It was used to cast a replica in PDMS (Sylgard 184, Dow Corning).

The flow in the microchannels was driven by setting differences in hydrostatic pressure between the inlets [ports

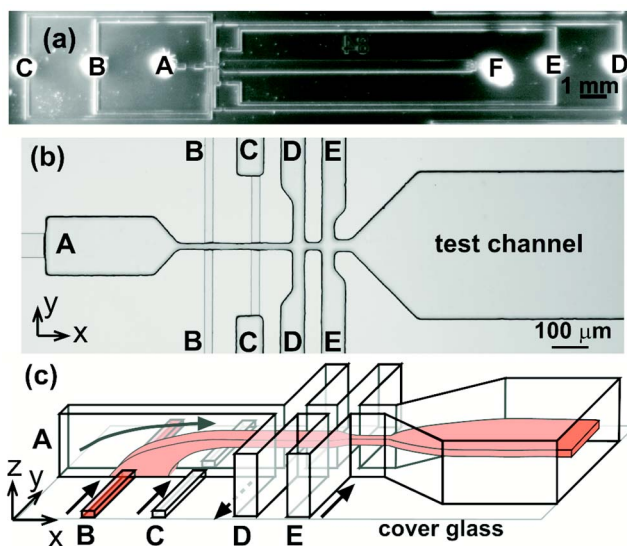


FIG. 1. (Color online) (a) Photograph of the microfluidic device. (b) Magnified image of its main functional area. (c) Schematic diagram showing structure of the flow in the device with the liquid injected from port  $B$  appearing in a dark color.

<sup>a)</sup> Author to whom correspondence should be addressed; electronic mail: [agroisman@ucsd.edu](mailto:agroisman@ucsd.edu)

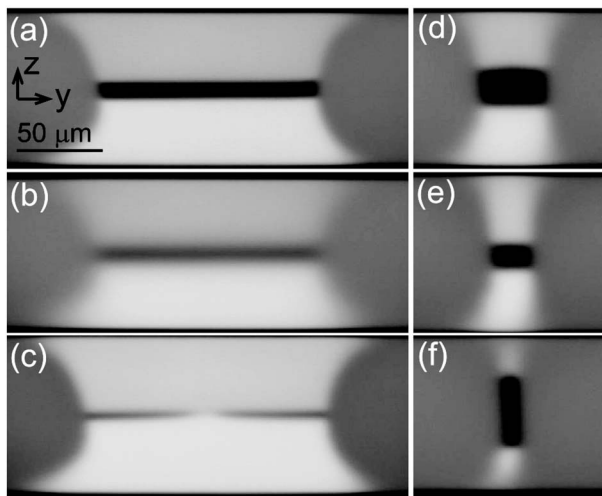


FIG. 2. Confocal micrographs showing distributions of fluorescent dye (FITCD) near the central axis of the test channel at different pressures at the device inlets. (a) and (c)–(f) were taken at the beginning of the test channel and (b) was taken near the end of it. Port *D* was blocked and differential pressures at ports *A*, *B*, *C*, and *E* in kPa with respect to port *F* were: (a), (b) 6.6, 9.7, 7.4, and 9.4; (c) 8.6, 6.9, 9.7, and 10.7; (d) 4.1, 5.9, 3.7, and 9.4; (e) 4.3, 4.6, 4.1, and 11.2; (f) 3.8, 4.8, 3.3, and 11.2.

*A*, *B*, *C*, and *E* in Fig. 1(a)] and outlets [ports *D* and *F* in Fig. 1(a)]. Normally, port *D* was either blocked or pressurized at a level resulting in zero flow through it, so that the liquid fed to all four inlets was directed to port *F*. The set-up for driving and controlling the flow is described in detail elsewhere.<sup>9</sup> The flow was always laminar and stable with  $Re < 1$ . Measurements of the distribution of fluorescent dye and particles injected into the flow were performed in the test channel (Fig. 1), which had depth, width and length  $h=100\ \mu\text{m}$ ,  $w=500\ \mu\text{m}$ , and  $l=10\ \text{mm}$ , respectively.

In order to visualize profiles of the streams of liquid fed to different inlets, we used solutions of fluorescein-conjugated Dextran (FITCD,  $M_w \cong 2\ \text{MDa}$  by Sigma) in a  $pH=7.5$  phosphate buffer. The solutions fed to the inlets *A*, *C*, and *E* had FITCD concentrations of 200, 240, and 120 ppm, respectively. The liquid fed to port *B* was a plain buffer without dye. The maximal flow velocity in the test channel,  $v_{\text{max}}$ , was  $\sim 4.5\ \text{mm/s}$ . Profiles of fluorescence across the test channel at various combinations of inlet pressures are shown in Fig. 2. They were taken with a confocal microscope (BioRad 1024) and a  $60\times/1.2\ \text{WI}$  objective. Brightness of fluorescence in various regions in Fig. 2(a) indicates that this profile corresponds to the flow schematically shown in Fig. 1(c). [We also measured the  $xz$  fluorescence profile along the symmetry plane of the tall-and-narrow channel using confocal imaging with a  $10\times/0.3$  objective, and it was consistent with the flow structure in Fig. 1(c) as well.] The liquid without dye is focused in the  $z$ -direction to the central 10% of the channel depth [Fig. 2(a)]. For a parabolic flow profile, its velocity is expected to be within 1% of  $v_{\text{max}}$ . Vertical and lateral dimensions of the stream from inlet *B* can be varied in a broad range by adjusting pressures at the inlets [Figs. 2(c)–2(f)].

In Fig. 2(c), the stream from inlet *B* is focused to the central 4% of the channel depth, so that its velocity is expected to be uniform within 0.2%. However, with this tight focusing along the  $z$ -axis, the stream does not have a regular shape and has a gap in the middle [Fig. 2(c)]. This irregular

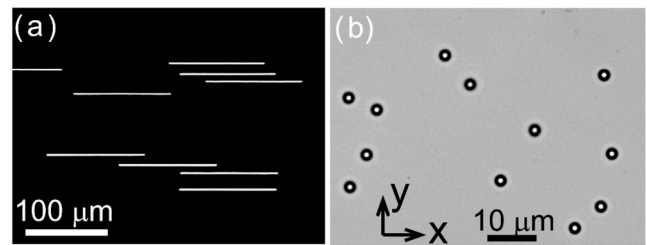


FIG. 3. (a) Fluorescence micrograph of streak lines produced by  $1.9\ \mu\text{m}$  fluorescent beads focused to  $\sim 4\ \mu\text{m}$  thick flow layer. (b) Bright field snapshot of  $2.5\ \mu\text{m}$  beads focused to  $2\text{--}3\ \mu\text{m}$  thick flow layer. Port *D* was blocked and differential pressures at ports *A*, *B*, *C*, and *E* in kPa with respect to port *F* were: (a) 2.4, 2.0, 2.8, and 2.9; (b) 1.4, 1.0, 1.5, and 1.8.

shape is due to the finite ratio of the depth of the tall-and-narrow channel to its width,  $\sim 6$  in the current design (Fig. 1). For the situation in Fig. 2(c), the volumetric rate of flow in channel *A* is  $\sim 10$  times higher than the total volumetric rate of flows injected from channels *B*. Under these conditions the assumption about injection from the bottom is not completely valid, and the profile of the focused flow [Fig. 2(c)] is reminiscent of one with injection from the sides.

Sharp boundaries between the streams at the beginning of the test channel [Figs. 2(a) and 2(c)–2(f)] are due to low diffusivity of the dye ( $D=7.8\times 10^{-8}\ \text{cm}^2/\text{s}$ ), moderately high flow rate and high resolution of the confocal imaging. The boundaries become smeared at the end of the channel [Fig. 2(b)]. The broadening of the horizontal boundaries is uniform, in contrast to the essentially nonhomogeneous boundary broadening in streams focused only laterally.<sup>10</sup> The width of the boundaries is consistent with the characteristic diffusion scale  $\sqrt{2Dt}=6\ \mu\text{m}$ , where  $t=l/v_{\text{max}}=2.2\ \text{s}$  is the residence time in the flow. Homogeneous initial conditions at the boundaries and direct connection of the residence time with the position along the channel make the device a promising tool for studying molecular diffusivity and kinetics of diffusion limited chemical reactions.

To test focusing of particles in the flow, we used suspensions of  $1.9\ \mu\text{m}$  green fluorescent beads (Bangs Labs) and  $2.5\ \mu\text{m}$  plain polystyrene beads (Polysciences) in a solution of 8% sucrose and 5% Dextran ( $M_w \cong 2.5\times 10^5$  by Polysciences) in water. The suspensions were fed to port *B* (Fig. 1) and the solution without beads was fed to the other inlets. The solution had viscosity of 4 cPs and its density closely matched the density of the beads, thus making them neutrally buoyant. The flow was photographed with a Spot RT-SE18 camera on a Nikon TE2000 inverted microscope. Figure 3(a) shows a fluorescence micrograph of the  $1.9\ \mu\text{m}$  beads taken with a  $20\times/0.7\ \text{WI}$  objective and exposure time of 0.35 s in a flow with  $v_{\text{max}}=0.35\ \text{mm/s}$ . The stream with the beads is focused into a  $\sim 4\ \mu\text{m}$  thick layer around the mid-plane of the test channel [cf. Fig. 2(c)]. We estimated bead velocities by measuring lengths of  $\sim 1000$  individual streak lines of the beads in a series of images with the same exposure time. The velocities were distributed with a standard deviation of 0.25%, part of which was due to some non-uniformity of the channel depth and measurement errors.

Figure 3(b) shows a representative micrograph of a stream with the  $2.5\ \mu\text{m}$  beads that is focused near the mid-plane to a flow layer estimated as  $2\text{--}3\ \mu\text{m}$  thick. The micrograph is taken at  $v_{\text{max}}=0.2\ \text{mm/s}$  under bright field illumination with an exposure time of 0.5 ms using a  $60\times/1.2\ \text{WI}$

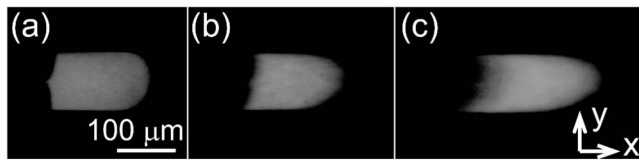


FIG. 4. Fluorescence micrographs of a  $\sim 7 \mu\text{m}$  thick blob of 2400 ppm FITCD solution taken with a  $20\times/0.7$  WI objective with 2 ms exposure: (a) at the beginning of the test channel, (b) 5 mm downstream, and (c) 10 mm downstream (at the end of the channel). Differential pressures at ports A, B, C, and E in kPa with respect to port F were 29.5, 38.1, 29.5, and 42.2. Differential pressure at port D was normally 14.7 kPa with no flow through port D, and in order to create the blob it was dropped to  $-1.5$  kPa for 150 ms two times with an interval of 180 ms.

objective with the depth of field of less than  $1 \mu\text{m}$ . Sharp images of the beads in Fig. 3(b) are consistent with the suggested tight focusing of the stream in the  $z$ -direction. Similar quality of flow focusing was achieved at  $v_{\text{max}}$  up to 2 cm/s (limited by deformation of PDMS at high driving pressures). We believe that with some modifications of the device to reduce flow resistance and prevent instabilities, and with a harder formulation of PDMS, the range of  $v_{\text{max}}$  can be expanded to 1–10 m/s, which is typical for commercial flow cytometers.<sup>2</sup>

The parabolic profile and high dispersion of velocity in pressure-driven flows impose some constraints on transport of chemicals and particles along microchannels. In particular, a blob of chemicals (or particles) injected into the flow rapidly spreads along the flow direction.<sup>11</sup> Therefore, delivery of desired volumes of chemicals through microchannels, which would be beneficial for lab-on-a-chip applications, is generally problematic. As it is shown in Fig. 4, the issue of axial dispersion is resolved by appropriate hydrodynamic focusing of the injected blob. A blob of FITCD, which appears as a bright spot in Figs. 4(a)–4(c), is focused in the  $z$ -direction to the central 7% of the channel depth and is moving with a speed of 5 mm/s. FITCD is dissolved at 2400 ppm in a 5% solution of Dextran ( $M_w \cong 2.5 \times 10^5$  by Polysciences) in a  $\text{pH}=9$  buffer and is fed to port B. A plain Dextran solution is fed to ports A, C, and E [cf. Fig. 1(c)]. The viscosity of the solution is about 3.7 cPs, which reduces the diffusivity of FITCD to  $2 \times 10^{-8} \text{ cm}^2/\text{s}$  (suggesting that  $D \sim 1/\eta$ ). The blob is generated by two consecutive short drops of pressure at port D. The pressure is reduced to a level that diverts the whole flow from ports A, B and C to port D, while the liquid from port E keeps flowing through the test channel towards

port F (Fig. 1). One can see that the blob remains essentially confined even after traveling a distance  $l=100 \cdot h$  [Fig. 4(c)]. The axial smearing of the blob [length of the tail in Fig. 4(c)] is about  $80 \mu\text{m}$ , which is consistent with dispersion of flow velocity across the blob in the  $z$ -direction. The rounding of the leading edge of the blob at the end of the channel [Fig. 4(c)] is due to finite  $w/h$ , which leads to some nonhomogeneity in the velocity profile along the  $y$ -direction.

In summary, we demonstrated tight 2D hydrodynamic focusing in a simple microfluidic device, which is made of a single cast of PDMS using soft lithography with no assembly required. The velocity distribution of particles in the focused stream is very narrow, with a standard deviation as low as 0.25%. The device is fully compatible with the regular microscope objectives and could be a low cost alternative for flow cytometry systems. Multiple copies of the device can be made with high fidelity by molding, and it can be easily combined with other microfluidic elements. Large flexibility in shaping the profile of the focused stream (Fig. 2) may make the proposed device suitable for additional optical testing configurations and techniques. Finally, the transport of confined blobs of chemicals through the microchannel should make the 2D flow focusing element [Fig. 1(c)] a useful component for integrated lab-on-a-chip systems.

The authors thank D. Kleinfeld and C. Schaffer for useful discussions and V. Vandelinder for valuable comments. The project was partially supported by NSF Grant No. OCE 04-28900.

<sup>1</sup>P. Crosland-Taylor, *Nature (London)* **171**, 37 (1953).

<sup>2</sup>M. A. Van Dilla, *Flow Cytometry: Instrumentation and Data Analysis* (Academic, London, 1985).

<sup>3</sup>G. M. Whitesides, E. Ostuni, S. Takayama, X. Y. Jiang, and D. E. Ingber, *Annual Review of Biomedical Engineering* **3**, 335 (2001).

<sup>4</sup>J. B. Knight, A. Vishwanath, J. P. Brody, and R. H. Austin, *Phys. Rev. Lett.* **80**, 3863 (1998).

<sup>5</sup>S. Takayama, E. Ostuni, P. LeDuc, K. Naruse, D. E. Ingber, and G. M. Whitesides, *Nature (London)* **411**, 1016 (2001).

<sup>6</sup>S. Eyal and S. R. Quake, *Electrophoresis* **23**, 2653 (2002).

<sup>7</sup>N. Sundararajan, M. S. Pio, L. P. Lee, and A. A. Berlin, *J. Microelectromech. Syst.* **13**, 559 (2004).

<sup>8</sup>R. Yang, D. L. Feebback, and W. J. Wang, *Sens. Actuators, A* **118**, 259 (2005).

<sup>9</sup>A. Groisman, M. Enzelberger, and S. R. Quake, *Science* **300**, 955 (2003).

<sup>10</sup>R. F. Ismagilov, A. D. Stroock, P. J. A. Kenis, G. Whitesides, and H. A. Stone, *Appl. Phys. Lett.* **76**, 2376 (2000).

<sup>11</sup>G. I. Taylor, *Proc. R. Soc. London, Ser. A* **219**, 186 (1953).